Cellulose (2020) 27:7139–7155
https://doi.org/10.1007/s10570-020-03282-8

ORIGINAL RESEARCH

Recyclable photocatalyst composites based on Ag_3VO_4 and Ag_2WO_4 @MOF@cotton for effective discoloration of dye in visible light

Hossam E. Emam · Hanan B. Ahmed · Eslam Gomaa · Maher H. Helal · Reda M. Abdelhameed

Received: 6 April 2020 / Accepted: 3 June 2020 / Published online: 11 June 2020

Abstract Photocatalysts are highly applicable in treatment of the water pollution. However, most of the applied photocatalysts suffer from the inapplicability and non-recyclability which limited their application. Herein, applicable and recyclable effective photocatalyst composites of Ag_2WO_4@MIL-125-NH_2@cotton and Ag_3VO_4@MIL-125-NH_2@cotton successfully prepared by direct synthesis of MIL-125-NH_2 and Ag_2WO_4 or Ag_3VO_4 within the cotton fabric as supported template, sequentially. Agglomerated rock structure of Ag_2WO_4@MIL-125-NH_2 and smaller particles of Ag_3VO_4@MIL-125-NH_2 formed onto the cotton. The prepared composites applied as photocatalysts in the degradation of Methylene Blue (MB) and Rhodamine B (RhB) dyes in the visible light. The highest photodegradtion of dyes observed for Ag_2WO_4@MIL-125-NH_2@cotton and Ag_3VO_4@MIL-125-NH_2@cotton composites because of their low optical band gaps (2.36 eV and 1.87 eV) and their quenching in luminescent spectrum which helped in the ease transfer of photoexcited electrons. The rate constant (k_2) for the photodegradation of MB (RhB) dye reduced significantly from 1.78×10^{-3} (2.8×10^{-3}) L/mg min to 0.43×10^{-3} (1.04×10^{-3}) L/mg min and 0.29×10^{-3} (0.79×10^{-3}) L/mg min, when Ag_2WO_4 and Ag_3VO_4 incorporated in MIL-125-NH_2@cotton composite, respectively. After 4 recycling process, the photodegradation activity of the applied composites diminished from 86–92% (68–80%) to 58–65% (47–54%). The obtained results declared the topmost photocatalytic activity in daylight of the recyclable prepared tri-component composites, reflecting their promising potentials in environmental applications.

Electronic supplementary material The online version of this article (https://doi.org/10.1007/s10570-020-03282-8) contains supplementary material, which is available to authorized users.

H. E. Emam (✉)
Textile Industries Research Division, Department of Pretreatment and Finishing of Cellulosic Based Textiles, National Research Centre, Scopus affiliation ID 60014618, 33 EL Buhouth St., Dokki 12622, Giza, Egypt
e-mail: hossamelemam@yahoo.com

H. B. Ahmed (✉) · E. Gomaa · M. H. Helal
Chemistry Department, Faculty of Science, Helwan University, Ain-Helwan 11795, Cairo, Egypt
e-mail: hananabasiony@gmail.com

R. M. Abdelhameed (✉)
Chemical Industries Research Division, Applied Organic Chemistry Department, National Research Centre, Scopus affiliation ID 60014618, 33 EL Buhouth St., Dokki 12622, Giza, Egypt
e-mail: reda_nrc@yahoo.com

Graphic abstract

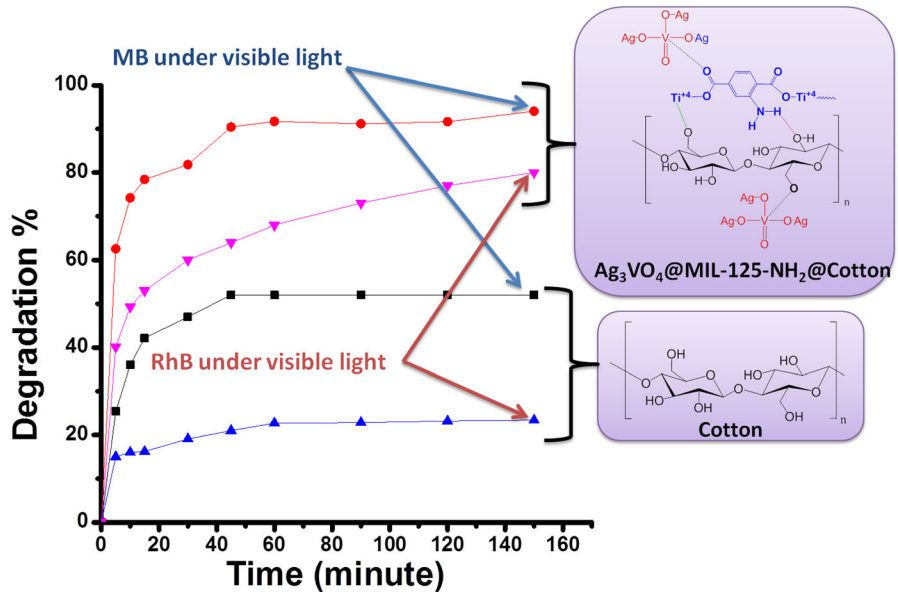

Keywords Cotton · Ag_3VO_4 · Ag_2WO_4 · MIL-125-NH_2 · Recyclable photocatalyst · Dye discoloration · Visible light

Introduction

Discharging of organic pollutants causes health problems to the local population (Garfield 2002). Organic pollutants could be classified to three categories: (i) hydrocarbons such as the polycyclic aromatic hydrocarbons, (ii) oxygen, nitrogen and phosphorus compounds and (iii) organometallic compounds (Connell and Miller 1984). The major category is the hydrocarbons (especially aromatic polycyclic compounds, such like dye stuffs and commercial colorants), with chemical bonds which are relatively stable bonds and have limited polarity. They will be adsorbed by sediment and bio-coagulated in fatty tissues of organisms and consequently disrupt the endocrine system (Forbes 1993). These cause hormonal system to be disrupted, causing reproductive problems, additionally, these compounds are often carcinogens (Connell et al. 2009; Connell 2005). Due to their widely discharged from industrials sectors like, textile, plastic and pharmaceuticals, dyes considered the most aromatic polycyclic pollutants released into the environment. Besides their toxic effect, colorants prevent the penetration of sunlight to the aqua organisms which shows hazardous environmental effects (Jones and De Voogt 1999; Landis et al. 2003; Francis 1994). Therefore, removal or discoloration of organic dyes from the wastewater is an important issue for protection of the living organisms and environment (Ahmed et al. 2020; Emam et al. 2020).

Several methods were employed for removal/discoloration of dyes such as adsorption, ultrafiltration, chemical and electrochemical methods, and biological treatment (Ahmed et al. 2020; Emam and Ahmed 2019; Emam and Shaheen 2019; Panakoulias et al. 2010; Ghoreishi and Haghighi 2003). The employment of adsorbents for removal of organic pollutants like dyes involves phase transfer without its decomposition and thus induces another pollution (Zhou et al. 2015; Wankhade Atul et al. 2013). Chemical oxidation is unable to mineralize all dyes and is only economically favorable for removing of high concentrations of pollutants (Rasalingam and Peng 2014; El-Dein et al. 2006). While, for application of biological treatment, the main disadvantages are slow reaction rates, disposal of sludge and requirement for controllable pH and temperature (Ghoreishi and Haghighi 2003). Hence, degradation/discoloration of dyes has gained considerable interest and subsequently using of

photocatalyst considered as a big challenge in order to reduce the chemical pollution and energy consumption. A lot of recent works focused on preparation of photoactive catalysts based on materials such like, TiO_2, ZnO, Ag_3PO_4, $AgVO_3$, KSbPON, ZrP/AgBr, Fe_2O_3, $Bi2MoO_6$, and metal organic frameworks were reported (Balu et al. 2018; Abdelhameed et al. 2015; Abdelhameed et al. 2018b; Sitthichai et al. 2017; Bibi et al. 2018; Zhou et al. 2018; Ravi et al. 2016; Chekir et al. 2016; Gajbhiye 2012; Byrappa et al. 2006; Pica et al. 2019; Alshammari et al. 2014). Additionally, synthesis of composites based on bismuth vanadate ($BiVO_4$/$FeVO_4$@rGO, $BiVO_4$/$BiPO_4$/GO, Co_3O_4-$BiVO_4$/g-C_3N_4, CoO/$BiVO_4$) exhibited highly photocatalytic ability (Yang et al. 2020; Wang et al. 2019, 2020a, b). The ideal properties for any photocatalyst could be suggested as; suitability towards visible or near UV light, stability toward photocorrosion, the biological and chemical inertness, cheapness and lack of toxicity (Bhatkhande et al. 2002). The stronger light absorber, the better photocatalyst, which characterized by a long lifetime of excited electron, and good charge transfer. Most of the aforementioned photocatalysts can't be recycled and/or don't be active in the visible light. The recyclability and photo-activation in the visible light are the two important issues which are highly required for the catalyst to be applied in the large scale. Limited work based on a recyclable photocatalyst composites containing cotton were recently prepared such as $BiVO_4$/SiO_2/reduced graphene oxide and Fe(III)@$BiVO_4$/-cotton (Liu et al. 2018; Zhang et al. 2019).

Metal organic frameworks (MOFs) are one from the active photocatalysts due to their effective band gap (Abdelhameed et al. 2015, 2017). However, an additional enhancement in their catalytic activity were carried out by incorporation of semiconductors or precious metals which helped in preventing the recombination between the excited electrons and produced holes (Abdelhameed et al. 2015; Xiang et al. 2017; Yang et al. 2017). According to our knowledge, no research approaches has been studied the photocatalysis of MOF containing composites loaded fabrics as recyclable photocatalyst. From that point forward, the current study presented a preparation of a new recyclable photocatalysts based on cotton fabrics as supported template by using a new simple technique. The composites were synthesized by direct formation of MIL-125-NH_2 and silver vanadate (Ag_3VO_4) or silver tungstate (Ag_2WO_4) within the cotton matrix. The prepared composites were characterized by scanning electron microscope, energy dispersive X-ray, X-ray diffraction and infrared spectroscopy. The photocatalytic activities of the composites studied via the degradation of Rhodamine B and Methylene blue dyes in the visible light. Both of kinetics and isotherm for the photodegradation of dyes were performed. The recyclability of the composites towards reusing process also were presented. The photocatalytic mechanism of the composites in dye degradation was suggested through studying the effect of the electron scavengers.

Experimental

Chemicals and materials

Titanium (IV) isopropoxide (97%), 2-aminoterephthalic acid (99%), silver nitrate ($\geq$ 99.9%), sodium hydroxide (99%), vanadium oxide (99.9%), sodium tungstate dehydrate ($\geq$ 99%), dimethylformamide (99.9%), ethanol (absolute, 99.9%), methanol (absolute, 99.9%), methylene blue (C.I.Nr. 52,015) and rhodamine B (C.I.Nr. 45,170) were all supplied from Sigma-Aldrich with an analytical grade and used without purification.

Desized, scoured and bleached plain-woven 100% cotton fabrics (160 gm/m^2) kindly supplied from El-Mahalla Company for Spinning and Weaving, El-Mahalla El-Kubra—Egypt. The impurities removed by washing the fabrics for 30 min at 50 °C by using 2 g/L nonionic detergent (Hospatal CV—Clariant) with material to liquor ratio of 1/50. Fabrics rinsed with tap water and then dried on air.

Preparation of photocatalyst composites

MIL-125-NH_2, Ag_2WO_4 and Ag_3VO_4 ingrown individually within the cotton fabrics according to the previously reported methods (Huang et al. 2009; Ramezani et al. 2015; De Santana et al. 2014; Abdelhameed and El-Shahat 2019). In case of MIL-125-NH_2, piece of cotton fabric (20 cm × 20 cm) immersed in 2-aminoterephthalic acid (5.5 mM) solubilized in dimethyl formamide (DMF)/methanol mixture (2:1 v/v) and the mixture stirred at room temperature for 15 min. Titanium isopropoxide

(3.4 mM) added to the mixture drop wisely forming yellowish colored fabric. After 1 h, the mixture placed in the oven at 80 °C for 2 h to complete the reaction. Afterwards, the treated fabric removed, washed with DMF followed by methanol and finally dried at 75 °C to obtain MIL-125-NH_2@cotton composite.

For incorporation of Ag_2WO_4 or Ag_3VO_4, cotton fabric pieces (20 cm × 20 cm) and MIL-125-NH_2@-cotton composite soaked individually in Na_2WO_4 (1.0 mM) or mixture from V_2O_5 (0.1 M) and NaOH (0.6 M) under stirring at room temperature, respectively. Then silver nitrate (0.3 M) added separately drop by drop forming greyish and yellowish colored fabrics, respectively. After stirring for 30 min, the mixtures kept in the oven at 80 °C for 2 h to complete the reaction. The treated fabrics and composites taken out, washed by distilled water and then dried at 75 °C. The prepared composites labeled as Ag_2WO_4@cotton, Ag_3VO_4@cotton, Ag_2WO_4@MIL-125-NH_2@cotton and Ag_3VO_4@MIL-125-NH_2@cotton composites.

Characterization

The morphological features of the prepared composite (MIL-125-NH_2@Cotton, Ag_2WO_4@Cotton, Ag_3VO_4@Cotton, Ag_3VO_4@MIL-125-NH_2@Cotton and Ag_2WO_4@MIL-125-NH_2@Cotton) sample investigated under a scanning electron microscope (SEM, Hitachi SU-70, running at 25 kV, Japan) at room temperature. The elemental analysis of samples performed by the field emission gun energy dispersive X-ray spectrometer analyzer, equipped with the same microscope. The diameter and dimensions of the prepared samples were calculated by using 4 pi analysis software using the micro-photos.

X-ray diffractograms for the prepared composites (MIL-125-NH_2@Cotton, Ag_2WO_4@Cotton, Ag_3VO_4@Cotton, Ag_3VO_4@MIL-125-NH_2@Cotton and Ag_2WO_4@MIL-125-NH_2@Cotton) measured by X'Pert MPD Philips diffractometer with monochromated Cu $K_\alpha$radiation (Cu Kα X-radiation at 45 kV, 40 mA and λ = 1.5406 Å). The diffraction performed in the 2θ region of 3.5°–80° at room temperature using 0.03° step size and rate of 2°/min.

The spectra of infrared for the prepared composites (MIL-125-NH_2@Cotton, Ag_2WO_4@Cotton, Ag_3VO_4@Cotton, Ag_3VO_4@MIL-125-NH_2@Cotton and Ag_2WO_4@MIL-125-NH_2@Cotton) measured by using Fourier transform infrared spectroscopy (FTIR, Mattson 5000 FTIR spectrometer). The instrument operated with attenuated total reflectance unite (ATR with Golden Gate diamond crystal). The absorption spectral data collected in the 500–4000/cm range.

UV–visible diffuse reflectance spectra through the composites detected by a JASCO spectrometer (USA). $BaSO_4$ used as a white reference powder.

Photoluminescent (PL) properties for the prepared composites measured by using Shimadzu, RF-5301 PC spectroflurophotometer at room temperature. The emission spectra of composites detected at excitation wavelength (λ_{ex}) of 460 nm.

Photocatalytic activity of composites

The photocatalytic activity of the prepared composites tested against the degradation of rhodamine B (RhB) and methylene blue (MB) dyes, in the visible light. The degradation process of dyes performed briefly as follows; a 100 mg of the composite (photocatalyst) immersed in 100 mL of dye solution (5 mg/L) under continuous stirring. In a closed chamber, the mixture irradiated by LED visible with lamp (12 W) as visible light source with adjusted temperature at 25 °C. The concentration of dyes before and after irradiation analyzed by a UV–Vis spectrophotometer (JASCO, V-630, USA). The percentage of dye degradation calculated by normalization the intensity of absorbance (C) at maximum wavelength (λ_{max}, 550 nm for RhB and 664 nm for MB) to the initial intensity of absorbance (C_0). The photocatalytic efficacy of the applied composite estimated as function of the dye degradation (C/C_0).

As a comparison with the photodegradation of dye in visible light and for confirmation the catalyzing effect of light in the degradation, the degradation/adsorption of dyes onto the composites studied in the dark (absence of light) at using the same conditions.

Results and discussion

MIL-125-NH_2, Ag_2WO_4 and Ag_3VO_4 synthesized individually within the cotton fabric matrix as shown in Fig. 1. Ag_2WO_4 and Ag_3VO_4 ingrown separately over MIL-125-NH_2@cotton. The hydroxyl groups in cotton fabrics bind the metal ions (Ti, W, V) through electrostatic or coordination linkage. Additionally hydrogen bonding between NH_2 of MOF and OH of

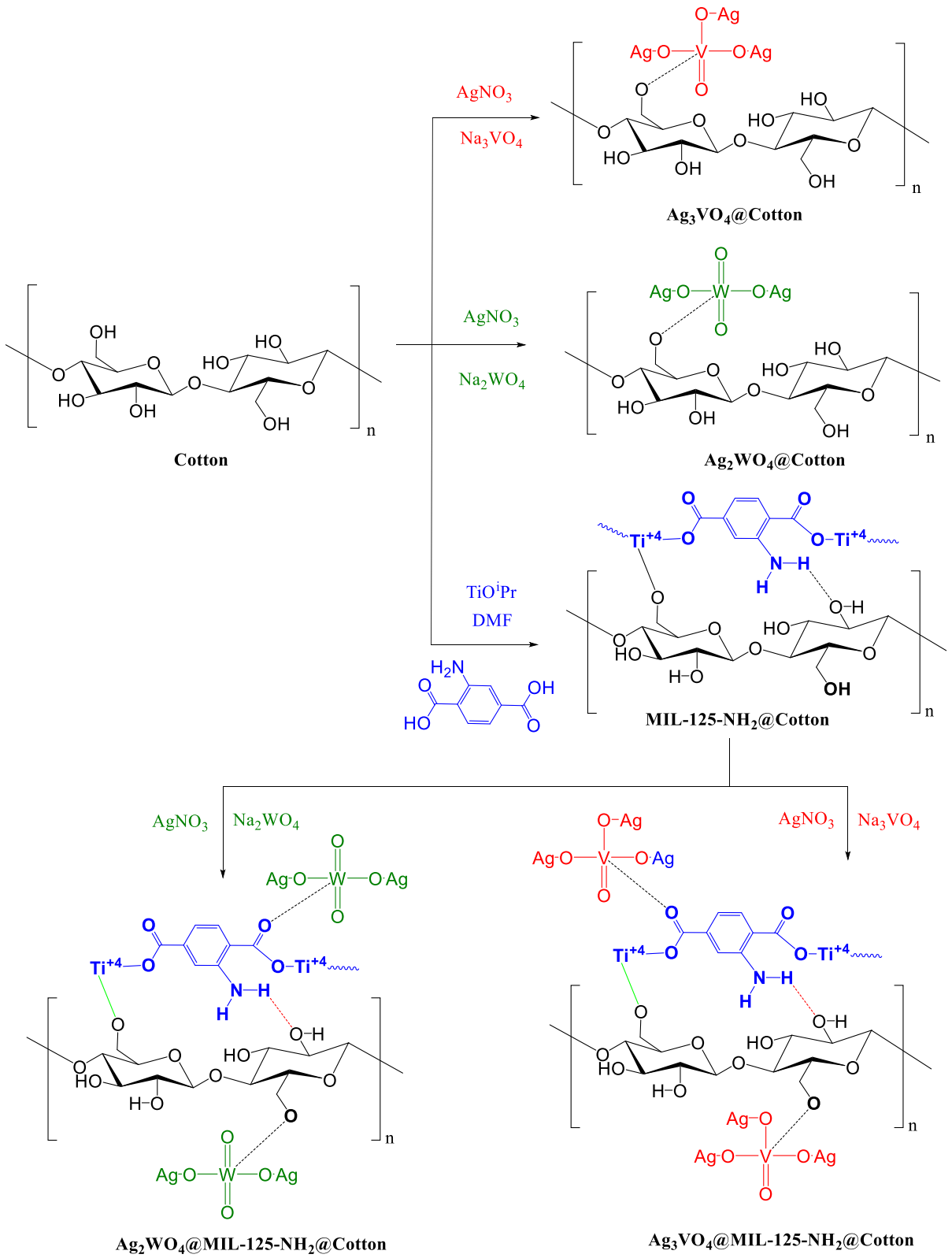
AgNO3
Na3VO4
Ag3VO4@Cotton
AgNO3
Na2WO4
Ag2WO4@Cotton
Cotton
TiOiPr
DMF
MIL-125-NH2@Cotton
AgNO3
Na2WO4
Ag2WO4@MIL-125-NH2@Cotton
AgNO3
Na3VO4
Ag3VO4@MIL-125-NH2@Cotton

◀**Fig. 1** Preparation mechanism of composites

cotton may form. In case of tri-components containing composites, linkage may form between MIL-125-NH_2 and silver tungstate or silver vanadate. In the next sessions, the all synthesized composites characterized by investigation of scanning microscope (SEM).X-ray diffraction (XRD), infrared (FTIR) and optical/photoluminescent properties.

Micrographs

The micrographs at three different magnifications and energy dispersive X-ray for the prepared composites (MIL-125-NH_2@Cotton, Ag_2WO_4@Cotton, Ag_3VO_4@Cotton, Ag_3VO_4@MIL-125-NH_2@Cotton and Ag_2WO_4@MIL-125-NH_2@Cotton) presented in Fig. 2. In case of the individual formation of materials, crystalline disc MIL-125-NH_2 in microsize formed on the surface of cotton. Meanwhile, spherical structures from Ag_2WO_4 and Ag_3VO_4 regularly observed onto cotton in nano dimension. The diameter size of Ag_2WO_4 and Ag_3VO_4 onto the fabrics ranged in 89 ± 16 nm and 197 ± 52 nm, respectively. The formation of the materials (MIL-125-NH_2, Ag_2WO_4 and Ag_3VO_4) within cotton fabrics confirmed by EDX analysis. Signals of Ti, Ag & W and Ag & V recorded besides the signals of C & O for cotton in case of the individual incorporation of MIL-125-NH_2, Ag_2WO_4 and Ag_3VO_4, respectively. These data are in agreement with literature for the individual prepared powder of MIL-125-NH_2, Ag_2WO_4 and Ag_3VO_4 (Zhao et al. 2017; Liu et al. 2019; Ramezani et al. 2015; Abdelhameed et al. 2018a; Emam and Abdelhameed 2017).

In case of incorporation of bi-components within cotton, both of the crystalline disc structure of MIL-125-NH_2 and the spherical shaped structure of Ag_2WO_4 and Ag_3VO_4 disappeared. Agglomerated rock like structure from Ag_2WO_4@MIL-125-NH_2 seen on the cotton, while, particles of Ag_3VO_4@-MIL-125-NH_2 formed onto cotton with smaller size. The synthesis of the bi-components within fabrics affirmed by the EDX analysis, as signals of Ti & Ag & W and Ti & Ag & V appeared beside signals of cotton for the incorporation of Ag_2WO_4@MIL-125-NH_2 and Ag_3VO_4@MIL-125-NH_2 inside the cotton matrix. SEM observation data confirmed the in-situ formation of the mono component (MIL-125-NH_2, Ag_2WO_4, Ag_3VO_4) and bi-components (Ag_2WO_4@MIL-125-NH_2, Ag_3VO_4@MIL-125-NH_2) within the network of cotton fabrics to produce tri-components composites.

XRD data

X-ray diffractograms for the prepared composites displayed in Fig. 3. Cotton fabrics, exhibited three diffraction patterns at $2\theta° = 14.6°$, 16.2° and 22.3° corresponding to the crystalline cellulose I (Emam and Bechtold 2015; Emam et al. 2018). For MIL-125-NH_2@cotton, the characterized diffraction peaks for MIL-125-NH_2 at $2\theta° = 6.8°$, 9.8°, 11.8° and 15.6°, detected besides that of cotton. In case of Ag_2WO_4@-cotton and Ag_3VO_4@cotton, four diffractions at $2\theta° = 26.7°$ and 29.8°, 31.5° 32.1° and two diffractions at $2\theta° = 30.9°$ and 32.4° appeared respectively, along with the diffractions of cellulose I. In case of the amalgamation of bi-components within cotton, the diffraction patterns of Ag_2WO_4 & MIL-125-NH_2 and Ag_3VO_4 & MIL-125-NH_2 reported for Ag_2WO_4@-MIL-125-NH_2@cotton and Ag_3VO_4@MIL-125-NH_2@cotton composites, respectively. According to literature (Zhao et al. 2017; Ramezani et al. 2015; Abdelhameed et al. 2018a; Emam and Abdelhameed 2017; Abdelhameed et al. 2015), the obtained diffractograms data proved the successful in-situ synthesize of the individual and bi-components based MIL-125-NH_2 Ag_2WO_4 and Ag_3VO_4 inside the cotton fabrics, and consequently further confirmed the preparation of bi-components and tri-components composites.

FTIR spectra

The chemical structure of the prepared composites investigated through detection of the functional groups by measurement the ATR-FTIR absorbance spectra (Fig. 4). Cotton fabrics as cellulosic materials exhibited five main absorption bands at 3332–3257, 2888, 1645, 1426 and 1026/cm. These bands characterized for the O–H stretching, aliphatic C–H asymmetric, C=O stretching, CH_2 scissoring and C–O stretching, respectively (Emam and Bechtold 2015; Emam et al. 2018). After incorporation of MIL-125-NH_2, new sharp absorption bands appeared at 1370–1532, 1251 and 770/cm. The new bands attributed to the symmetric and asymmetric stretching

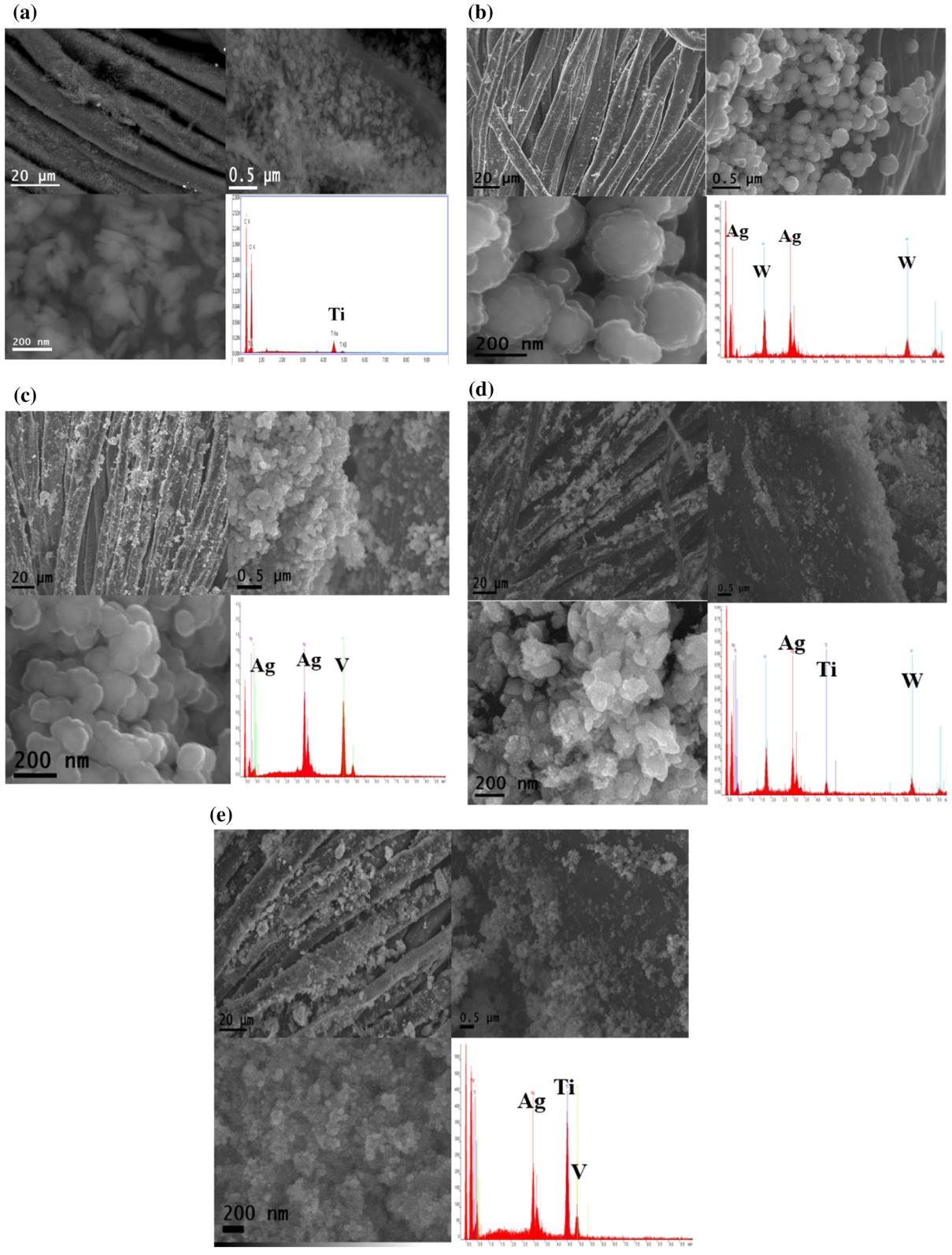
(a)
20 μm
0.5 μm
200 nm
Ti
(b)
20 μm
0.5 μm
200 nm
Ag
Ag
W
W
(c)
20 μm
0.5 μm
200 nm
Ag
Ag
V
(d)
20 μm
0.5 μm
200 nm
Ag
Ti
W
(e)
20 μm
0.5 μm
200 nm
Ag
Ti
V

◀**Fig. 2** Microscopic photos and EDX analysis for; **a** MIL-125-NH_2@Cotton, **b** Ag_2WO_4@Cotton, **c** Ag_3VO_4@Cotton, **d** Ag_2WO_4@MIL-125-NH_2@Cotton and **e** Ag_3VO_4@MIL-125-NH_2@Cotton

of O–C–O in carboxylate of organic acid ligand, the stretching of C–N aromatic amine in the ligand and the stretching Ti–O for metal organic framework (Abdelhameed et al. 2018a; Emam and Abdelhameed 2017; Vilela et al. 2017). Two new bands detected at 807–720/cm in case of the individual incorporation of Ag_2WO_4 and Ag_3VO_4, assigned for the stretching of W–O/V–O and Ag–O (Sreedevi et al. 2017; Ramezani et al. 2015; Zhao et al. 2017). For the incorporation of bi-components inside the fabrics, the absorption bands of both of MIL-125-NH_2 and Ag_2WO_4/Ag_3VO_4 observed clearly besides that of cotton. Those foundation of the spectral data supported the SEM and XRD results, and confirmed the successful formation of the desired materials within the cotton fabrics forming composites.

Optical and photoluminescence properties

The optical features of the synthesized composites performed through measurements of the absorbance spectra and the diffuse reflectance spectra presented in Fig. 5a. Cotton fabrics didn't show any absorption while, it exhibited absorbance peak at 395 nm after

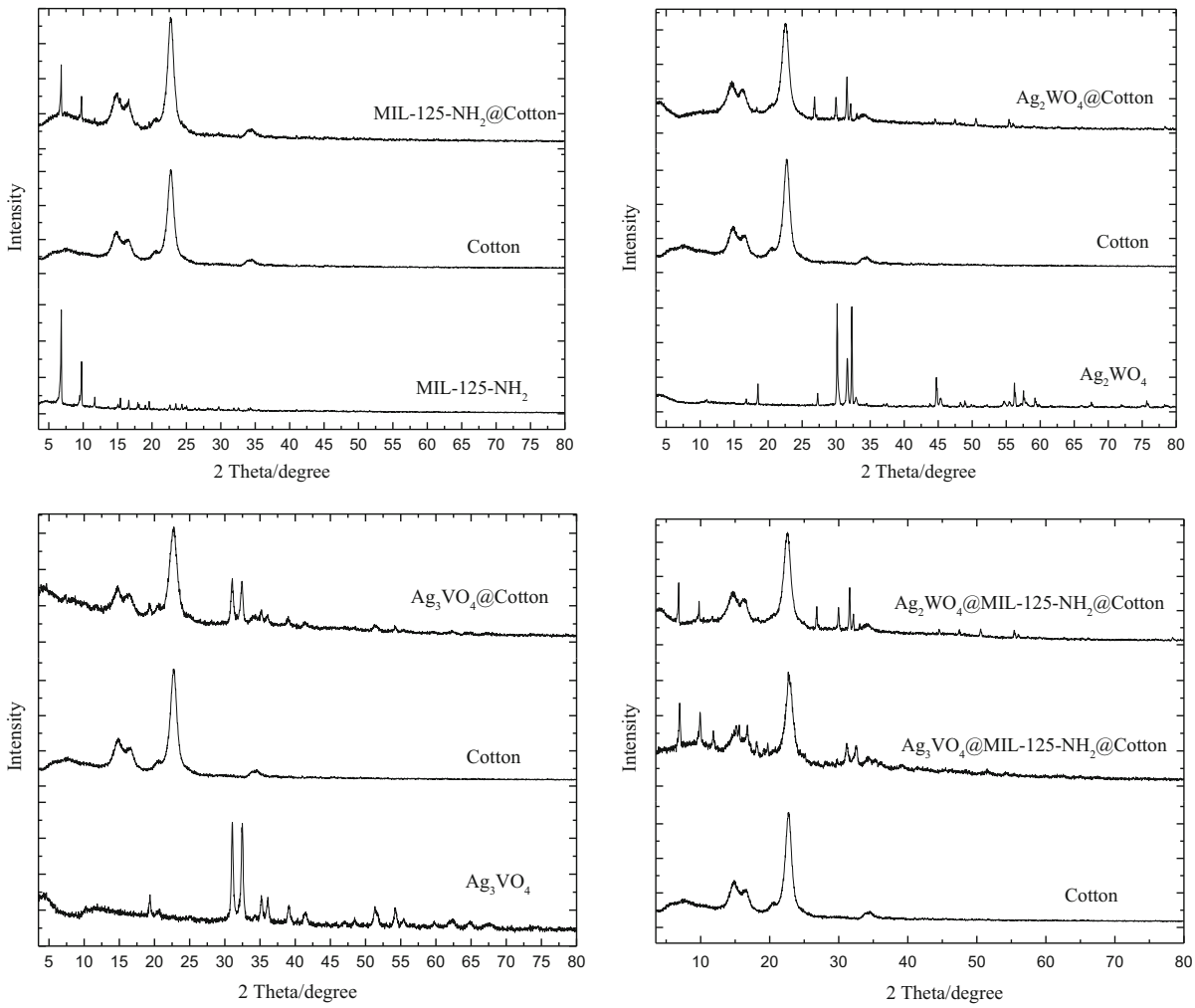

Fig. 3 X-ray diffractograms of cotton, MIL-125-NH_2, Ag_2WO_4, Ag_3VO_4, MIL-125-NH_2@Cotton, Ag_2WO_4@Cotton, Ag_3VO_4@-Cotton, Ag_2WO_4@MIL-125-NH_2@Cotton and Ag_3VO_4@MIL-125-NH_2@Cotton

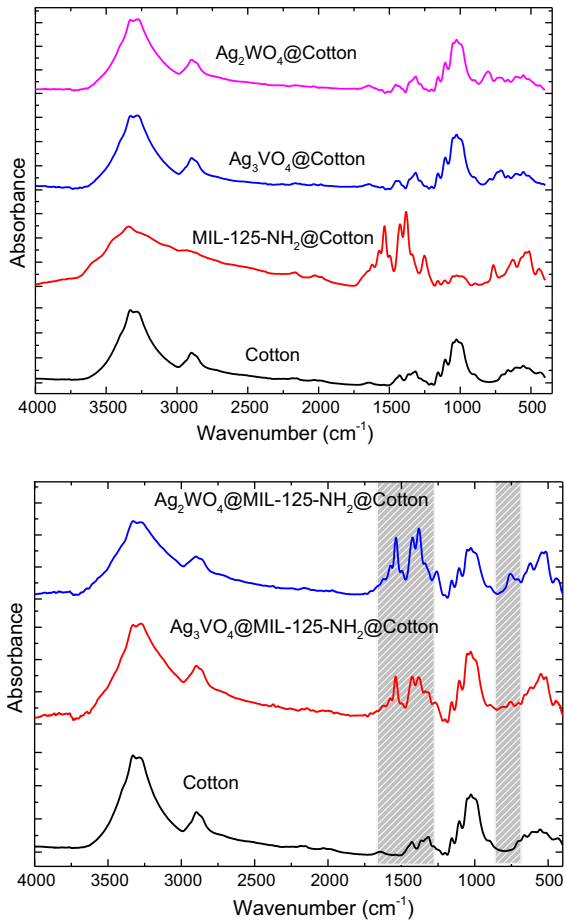

Fig. 4 FTIR spectra for MIL-125-NH_2@Cotton, Ag_2WO_4@-Cotton, Ag_3VO_4@Cotton, Ag_2WO_4@MIL-125-NH_2@Cotton and Ag_3VO_4@MIL-125-NH_2@Cotton

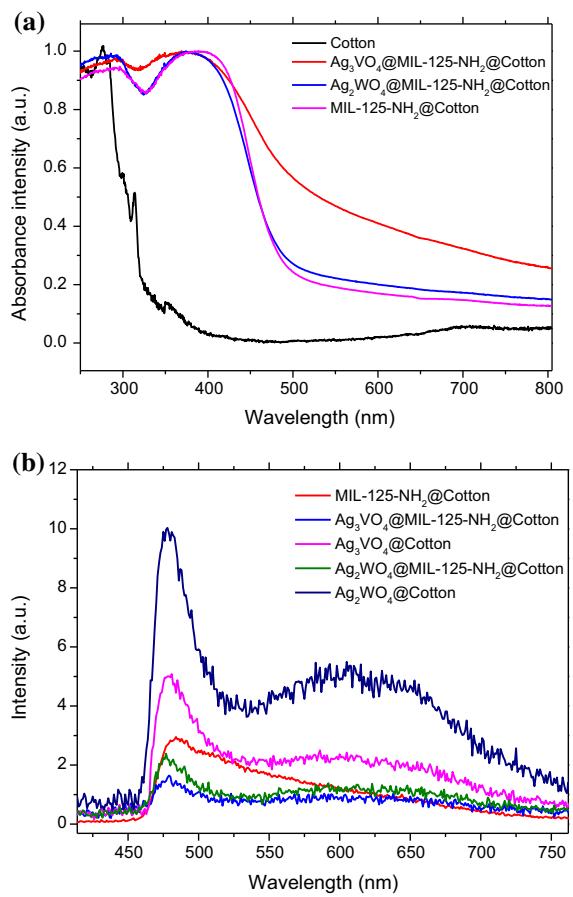

Fig. 5 Optical properties of the prepared composites; **a** absorbance spectra and **b** PL emission spectra at 460 nm excitation

incorporation of MIL-125-NH_2 which related to the charge transfer between metal and ligand (MLCT) (Hendon et al. 2013). After incorporation of Ag_2WO_4 and Ag_3VO_4, the fabrics showed individual absorbance peak at 385 nm and 404 nm, respectively. Considering the optical spectra for the single powder of the incorporated materials (Sreedevi et al. 2017; Hu et al. 2008), there is small shift (3–9 nm) in the absorbance peaks owing to the presence of cotton fabric. Additionally, the observed absorption tail in the visible region for the prepared composites indicating their catalytic activity in the visible light. By using the absorbance spectral data in Fig. 5 and the Tauc procedure, the optical band gabs (E_g) calculated for the all prepared composites (supplementary file, Fig. S1). The band gap values decreased from 2.46 eV for MIL-125-NH_2@cotton composite to 2.36 eV and to 1.87 eV for Ag_2WO_4@MIL-125-NH_2@cotton and Ag_3VO_4@MIL-125-NH_2@cotton composites, respectively. The reduction in band gap values of composite after incorporation of Ag_2WO_4 and Ag_3VO_4 declare the photocatalytic activity of the prepared composites in visible light.

The photoluminescence emission (PL) spectra after excitation at 460 nm for the all prepared composites measured and showed in Fig. 5b. The PL emission spectra for the MIL-125-NH_2@cotton showed a small peak. Whereas, an obvious PL emission peak at 482 nm and 476 nm recorded for Ag_2WO_4 & Ag_2WO_4@MIL-125-NH_2@cotton and Ag_3VO_4 & Ag_3VO_4@MIL-125-NH_2@cotton composites, respectively. The PL emission peaks in the composites corresponded to Ag_2WO_4 and Ag_3VO_4. This PL spectra declare that Ag_2WO_4@MIL-125-NH_2@cotton and Ag_3VO_4@MIL-125-NH_2@cotton able to

excite and emit in the visible light. Hence, the electron inside these composites can easily transfer from valence to conduction band in the visible light and consequently further confirmed their catalytic activity in the daylight.

The intensities of PL spectrum reduced from MIL-125-NH_2@cotton to Ag_2WO_4@MIL-125-NH_2@cotton and then to Ag_3VO_4@MIL-125-NH_2@cotton. This explained that the incorporation of Ag_2WO_4 and Ag_3VO_4 acted as traps for electron and transfer it to the adsorbed oxygen which acts as electron acceptor. Therefore, the quenching in PL spectrum reflected the ease transfer of photoexcited electron and resulted in improving the photocatalytic efficacy (Hu et al. 2008). The highest quenching in PL showed for Ag_3VO_4@MIL-125-NH_2@cotton displays its highest catalytic efficiency in visible light.

Photocatalytic activities

The catalytic efficiency of the prepared composites studied for MB and RhB dyes in the dark and visible light. The discoloration of dyes in the dark corresponded to adsorption of dyes onto the surface of materials. While the catalytic activity of the prepared composites studied in the visible light due to the degradation of dyes under photo-activation. The adsorption and degradation of dyes monitored via the reduction in their base absorbance peaks (665 nm for MB and 554 nm for RhB) and then calculated the percentage of adsorbed/degraded dyes as function of time. The data in Fig. 6a, c and supplementary file (S2) showed that, after 150 min under dark conditions, the adsorption capacity (percentage) of MB and RhB dyes onto the applied materials were 71.0–171.2 mg/g (14–34%) and 62.5–126.6 mg/g (12.5–25%). The adsorption capacity of dyes depended on the applied materials. The functional groups of cotton fabrics and pores of MIL-125-NH_2 are the main responsible for dye adsorption onto the applied composites.

Meanwhile, the irradiation of dye solutions under the visible light (Fig. 6b, d and S1), enhanced the discoloration of dyes significantly and the discoloration amount (percentage) were 260–458.5 mg/g (52–92%) and 113.5–340 mg/g (22.7–68%) for MB and RhB, respectively within only 60 min. The discoloration of dyes grown gradually with the irradiation time and was very rapid in the first 15 min. The MB discoloration was quite faster than that of RhB dye. The dye discoloration followed the order of cotton < Ag_3VO_4@cotton < Ag_2WO_4@cotton < MIL-125-NH_2@cotton < Ag_2WO_4@MIL-125-NH_2@cotton < Ag_3VO_4@MIL-125-NH_2@cotton. The lowest discoloration observed for cotton fabrics which reflected the minor effect of dye adsorption comparing to the dye degradation. Due to their highest photocatalytic activity confirmed from PL results, Ag_3VO_4@MIL-125-NH_2@cotton composite showed the highest dye photodegradation and consequently exhibited the highest total dye discoloration.

The discoloration of MB (RhB) dyes improved frequently from 257 (110) mg/g for cotton to 370 (250) mg/g for MIL-125-NH_2@cotton to 428 (315) mg/g and 465 (345) mg/g for Ag_2WO_4@MIL-125-NH_2@-cotton and Ag_3VO_4@MIL-125-NH_2@cotton composites. Due to the incorporation of MIL-125-NH_2, Ag_2WO_4@MIL-125-NH_2 and Ag_3VO_4@MIL-125-NH_2, the discoloration of dyes in visible light enhanced by factor of 2- 2.3, 2.5–3.6 and 3.4–3.5, respectively. Considering the adsorption amounts of dyes onto the composites in the dark, the estimated amount of degraded MB (RhB) dyes became 211 (125) mg/g, 265 (228) mg/g and 326.5 (245) mg/g for the MIL-125-NH_2@cotton, Ag_2WO_4@MIL-125-NH_2@cotton and Ag_3VO_4@MIL-125-NH_2@cotton composites, respectively. Therefore, the photodegradation of dyes enhanced by 1.3 (1.8) times and 1.6 (1.9) times by incorporation of Ag_2WO_4 and Ag_3VO_4 within MIL-125-NH_2@cotton composite, respectively. The results of dyes degradation are in agreement with the optical and luminescence properties and further confirmed the higher photocatalytic activity of the prepared composites (Ag_2WO_4@MIL-125-NH_2@cotton and Ag_3VO_4@MIL-125-NH_2@cotton composites) in the visible light. This declared that the prepared composites able to degrade the dyes (MB & RhB) in sun light without needing of the UV-irradiation.

The kinetic properties of the dyes (MB and RhB) degradation studied using nonlinear model of pseudo first and pseudo second order models. Figures of first order models presented in supplementary file (Fig. S3). The parameters of kinetic including coefficient of determination (R^2), rate constants of reaction (k_1 and k_2) and half-time ($t_{1/2}$), collected in Table 1. Chai square test (x^2) calculated for both kinetic models to check the fitting data and included in Table 1.

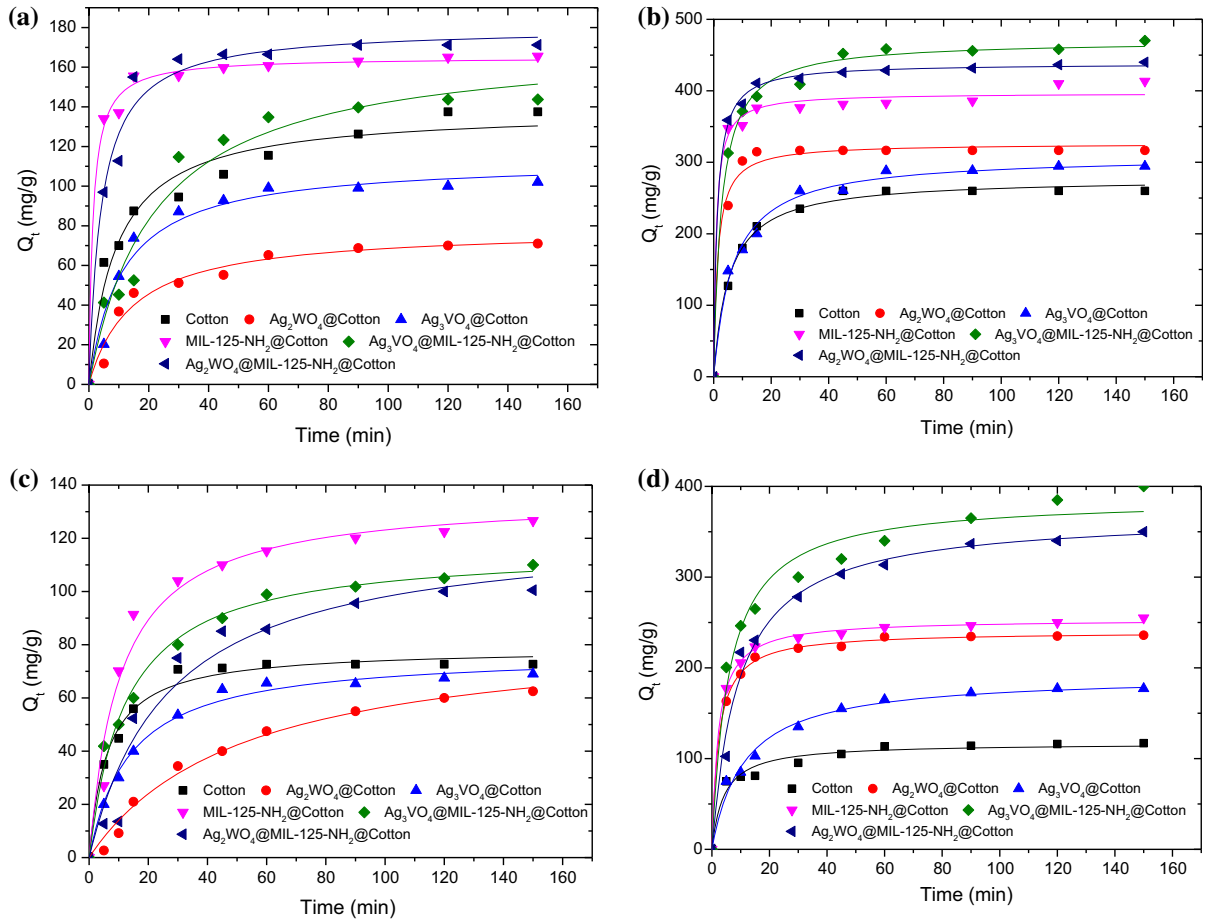

Fig. 6 Photocatalytic degradation of dyes at different irradiation time in presence of MIL-125-NH_2@Cotton, Ag_2WO_4@-Cotton, Ag_3VO_4@Cotton, Ag_2WO_4@MIL-125-NH_2@Cotton and Ag_3VO_4@MIL-125-NH_2@Cotton; **a**, **b** MB dye and **c**, **d** RhB dye, **a**, **c** in dark and **b**, **d** in visible light

Smaller values of x^2 and higher values of R^2 confirmed that the best fitting of dye degradation observed for pseudo second order model (Emam et al. 2018; Medhi and Bhattacharyya 2017). The estimated rate constant (k_2) for the photodegradation of MB and RhB dyes increased significantly from 2.97×10^{-3} L/mg min and 4.17×10^{-3} L/mg min for cotton to 17.8×10^{-3} L/mg min and 28.01×10^{-3} L/mg min for MIL-125-NH_2@cotton composite, respectively. By incorporation of Ag_2WO_4 and Ag_3VO_4 in the composite, the degradation rate constant further enlarged to 29.40×10^{-3} L/mg min and 36.20×10^{-3} L/mg min, for MB dye and 33.21×10^{-3} L/mg min and 41.84×10^{-3} L/mg min for RhB dye, respectively. The half time of MB (RhB) dye degradation significantly increased from 47.52 (66.7) min for cotton to 28.48 (44.80) min, 8.87 (18.64) min and 6.64 (12.41) min for MIL-125-NH_2@cotton, Ag_2WO_4@MIL-125-NH_2@cotton and Ag_3VO_4@MIL-125-NH_2@cotton composites, respectively.

Based on the data of kinetic parameters, the degradation time of MB and RhB dyes accelerated by factor of 4–5 times and 7–10 times, respectively when Ag_2WO_4@MIL-125-NH_2@cotton and Ag_3VO_4@MIL-125-NH_2@cotton composites applied as photocatalyst instead of cotton fabrics. The fastest degradation reaction of dyes observed for Ag_3VO_4@-MIL-125-NH_2@cotton composite, explained by its lowest band gap. The fitting of dye degradation reaction to second order kinetic model, reflected that, the degradation of dyes depends on two parameters; concentration of dyes and photocatalyst concentration.

Table 2 summarized the values for the half life time ($t_{1/2}$) of dyes (MB & RhB) in presence of different

Table 1 The kinetic parameters for the photocatalytic degradtion of dyes in the presence of the prepared composites

Dye	Catalyst	First order				Second order			
		K1 × 10^{-3} (min^{-1})	$t_{1/2}$ (min)	x^2	R^2	K2 × 10^{-3} (L/mg.min)	$t_{1/2}$ (min)	x^2	R^2
MB	Cotton	151.41	84.58	116.11	0.90	2.97	44.52	42.73	0.98
	MIL-125-NH_2@cotton	231.60	52.99	64.61	0.91	17.80	28.48	6.64	0.99
	Ag_2WO_4@cotton	220.41	33.14	130.42	0.96	16.20	22.92	46.51	0.99
	Ag_3VO_4@cotton	67.62	40.25	96.31	0.92	13.60	17.76	8.32	0.98
	Ag_2WO_4@ MIL-125-NH_2@cotton	83.84	18.27	1122.90	0.91	29.40	8.17	64.22	0.98
	Ag_3VO_4@ MIL-125-NH_2@cotton	119.52	15.80	345.53	0.88	36.20	5.84	81.50	0.98
RhB	Cotton	121.71	105.69	51.52	0.93	4.17	58.62	44.51	0.99
	MIL-125-NH_2@cotton	424.74	71.63	306.12	0.96	28.01	40.80	145.80	0.98
	Ag_2WO_4@cotton	285.82	42.43	314.71	0.92	22.20	34.2	109.21	0.98
	Ag_3VO_4@cotton	101.90	56.80	205.30	0.87	19.13	27.56	91.62	0.99
	Ag_2WO_4@ MIL-125-NH_2@cotton	339.11	24.04	198.90	0.95	33.21	12.64	24.62	0.99
	Ag_3VO_4@ MIL-125-NH_2@cotton	205.53	13.37	558.84	0.90	41.84	9.12	102.13	0.99

Table 2 Comparison between the half time for the photodegradation of dye by using different photocatalysts mentioned in literature

Dye	Photocatalyst	$t_{1/2}$ (min)	References
MB dye	Ag_3VO_4@ MIL-125-NH_2@cotton	5.8	Present study
	KSbPON (visible light)	68.0	Ravi et al. (2016)
	TiO_2 (visible light)	58.0–77.0	Chekir et al. (2016)
	ZnO (visible light)	9.0–26.0	Chekir et al. (2016
	ZnO (sun light)	18.0–51.0	Gajbhiye (2012))
	ZnS/CdS (visible light)	150.0–360.0	Soltani et al. (2012)
RhB dye	Ag_3VO_4@ MIL-125-NH_2@cotton	9.1	Present study
	KSbPON (visible light)	136.0	Ravi et al. (2016)
	TiO_2 (UV light)	24.9	Alshammari et al. (2014)
	ZnO (UV light)	34.1	Alshammari et al. (2014)
	Au/TiO_2 (UV light)	22.8	Alshammari et al. (2014)
	Au/ZnO (UV light)	12.7	Alshammari et al. (2014)
	ZnO (sun light)	18.5–31.7	Byrappa et al. (2006)
	ZrP/AgBr (sun light)	7.9	Pica et al. (2019)

catalysis which reported in literature. Photodegradation of both dyes (MB & RhB) in visible light needed quite longer time ($t_{1/2}$ = 68.0–360.0 min) at using of KSbPON and ZnS/CdS (Ravi et al. 2016; Soltani et al. 2012). While much diminished half time estimated for photodegradation of dyes in presence of TiO_2, ZnO, Au/TiO_2 and TiO_2/Zn (Alshammari et al. 2014; Byrappa et al. 2006; Chekir et al. 2016; Gajbhiye 2012) but still greater than that the ones detected for Ag_3VO_4@MIL-125-NH_2@cotton composites. Compared to the present prepared composite, similar half time recorded for RhB photodegradation when ZrP/AgBr applied (Pica et al. 2019). Therefore, the current prepared composite (Ag_3VO_4@MIL-125-

NH_2@cotton) exhibited much better catalytic activity compared to the other mentioned photocatlysts in Table 2. In addition to the prepared composite showed as recyclable to be widely applicable in environmental application than the referred photocatalyst powder.

Study of recyclability

The recyclability of the photocatalyst composites (Ag_2WO_4@MIL-125-NH_2@cotton and Ag_3VO_4@-MIL-125-NH_2@cotton) studied to perform the reusing ability towards the photodegradation of dyes. After the first using cycle, the photocatalyst composites isolated from dye solution by centrifugation and washed by distilled water followed by ethanol to remove the adsorbed dye. The washed photocatalyst composites dried at room temperature and then reuse again in the next degradation cycle. The process repeated four times to obtain five reusing degradation cycles and the reusing results presented in Fig. 7. The photodegradation of dyes diminished progressively by recycling process due to the release of the photoactive compounds (Ag_2WO_4@MIL-125-NH_2 & Ag_3VO_4@MIL-125-NH_2) from the cotton fabrics during the recycling process. However, the efficient of the applied composites still substantially good after 5 reusing times. The percentage of dyes photodegradtion lowered from 86–92% and 68–80% to 58–65% and 47–54% for MB and RhB, respectively after 4 reusing times. Therefore, the synthesized composites (Ag_2WO_4@MIL-125-NH_2@cotton and Ag_3VO_4@MIL-125-NH_2@cotton) can apply in the degradation of dyes in sunlight with significant reusing ability as recyclable photocatalyst. Besides their good photocatalytic activity, the applied

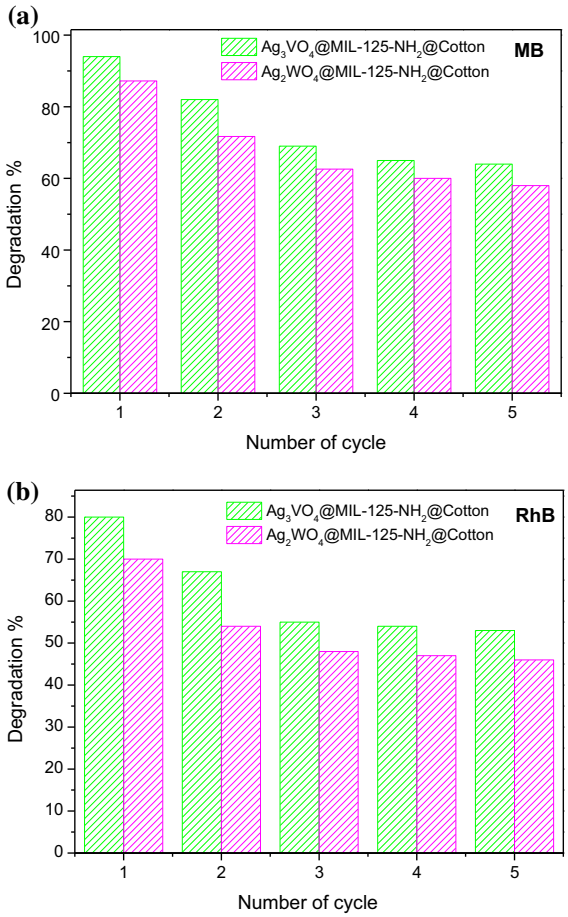

Fig. 7 Recycling efficiency of the photocatalyst on the degradation of dye in visible light; **a** MB and **b** RhB

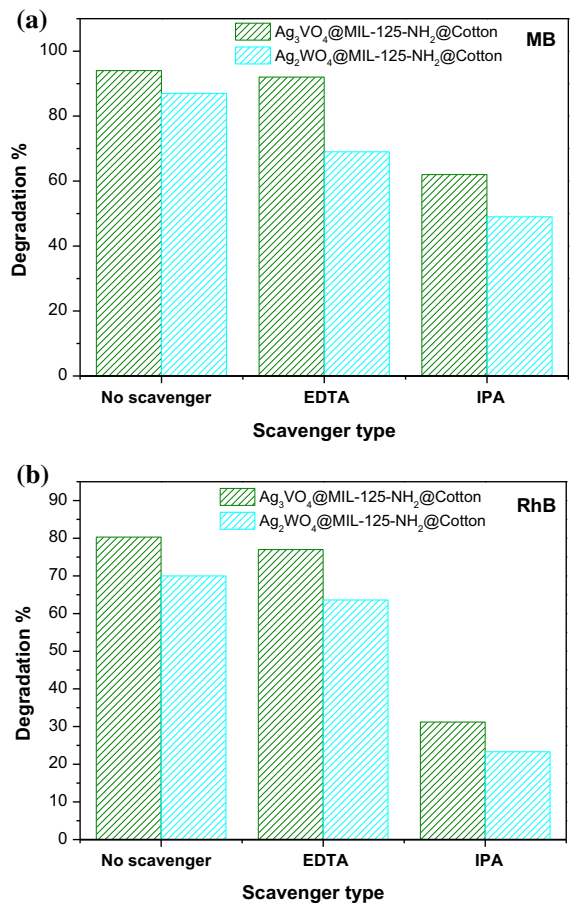

Fig. 8 Photocatalytic degradation of dye in visible light with different scavengers; **a** MB and **b** RhB

composites characterized by the recyclability compared to the others photocatalysts used in literature (Alshammari et al. 2014; Byrappa et al. 2006; Chekir et al. 2016; Gajbhiye 2012; Pica et al. 2019; Burgeth and Kisch 2002; Suresh et al. 2015; Neena et al. 2018).

Photo-degradation mechanism

The degradation of dyes under visible light was catalytically carried out in the presence of the prepared photocatalyst composites. As it was pre-mentioned, MOF is mainly constructed of metal in core which is coordinated to organic ligand. Taking in account that, the outer orbital of metal are the empty conduction band while the outer orbital of organic ligand is the valence band. As one of MOF, MIL has narrow band gap. Therefore, when the composite of MIL-125-NH_2@cotton, exposed to visible light, while the light energy equal or greater than the band gap of MIl, the electron–hole pairs formed, as the electrons (e^-) excited from the valence band (outer orbitals of organic ligand in MOF) leaving holes (h^+) to the conduction band (the empty outer orbitals of Ti) (Zhang and Lin 2014; Ma et al. 2012; Zhang et al. 2013). The photocatalytic activity of MOF can occur by the action of electrons or holes (Zhang et al. 2013; Zhang and Lin 2014). The holes (h^+) assumed to react with H_2O molecules or hydroxyl ions (^-OH) producing hydroxyl radicals (·OH), which oxidize the colored dye to colorless fragments. The excited electrons (e^-) may immediately entrapped by the dissolved O_2 in water forming superoxide radicals ($\cdot O_2^-$), which oxidize the dye species to uncolored fragments.

When Ag_2WO_4 or Ag_3VO_4 was inserted in the MIL-125-NH_2@cotton composite, the photo-catalytic activity was enhanced via the retardation effect for the recombination of hole/electron pair which is supposed to take a place in case of MIL-125-NH_2@cotton composite (Zhang et al. 2013; Zhang and Lin 2014). The excited electrons in the conduction band of MOF were transferred rapidly to the valence band of Ag_2WO_4 or Ag_3VO_4 and then to their conduction band. This electron jumping pathway which is commonly known as Z-scheme, is suggested to inhibit the

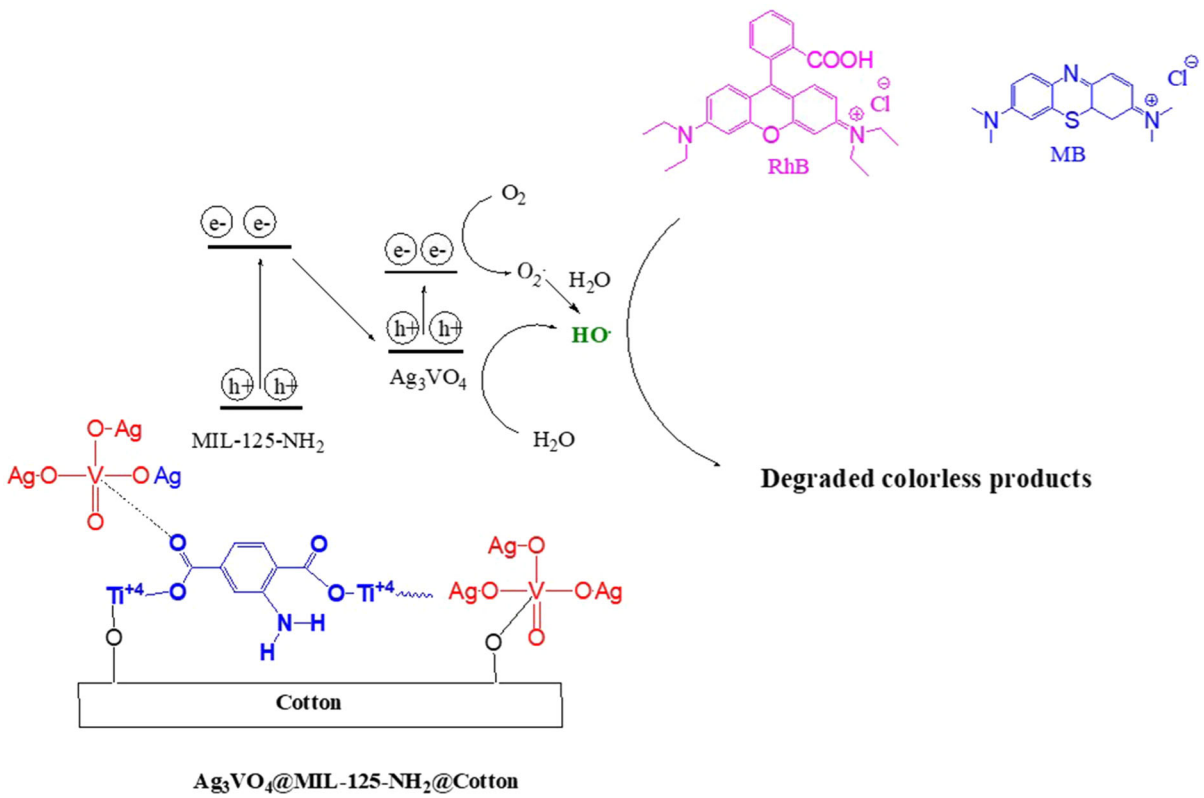

Fig. 9 Mechanism of photocatalytic degradation of dyes by the prepared composites

recombination process (Gao et al. 2019; Di et al. 2019). The separation between the generated carriers of charges is quite enough to prevent the recombination and further improved the photocatalytic action (Gao et al. 2019; Di et al. 2019; Seery et al. 2007). Moreover, the Ag_2WO_4 or Ag_3VO_4 may help in the excitation of electrons by enhancing the electric field through the formation of a local electric field (Seery et al. 2007).

The photocatalytic degradation of dyes by action of the composites (Ag_2WO_4@MIL-125-NH_2@cotton & Ag_3VO_4@MIL-125-NH_2@cotton) studied in the presence of scavengers to check the dye oxidation achieved by radical or holes. Figure 8 shows using of two different scavengers; isopropanol (IPA) and ethylenediaminetetraacetic acid (EDTA). IPA trapped the hydroxyl radicals (·OH) and EDTA block the holes (h^+). There wasn't notable changing in the dye photodegradation when EDTA used, meanwhile, significant lowering in photodegradtion of dyes observed in case of suing IPA. This confirms that, the hydroxyl radical (·OH) is the main responsible for oxidation of dyes. The generated holes in the valence band of Ag_2WO_4 or Ag_3VO_4 inside the composites may react with the hydroxyl ions ($^-$OH) to produce ·OH, as powerful oxidizing agent (Chin et al. 2018). Consequently, ·OH oxidize the dyes macromolecules and destroy the all conjugated system to produce colorless fragments (Fig. 9).

Conclusions

Recyclable effective photocatalysts based on cotton fabrics as supported template successfully synthesized by direct formation of MIL-125-NH_2 and Ag_2WO_4 or Ag_3VO_4 within the fabric matrix, consecutively. The produced composites investigated and confirmed by SEM, EDX, XRD and FTIR. To estimate their photocatalytic activities, the optical and luminescent properties of the composites studied. The photocatalytic activity of the prepared composites followed up in the degradation of MB and RhB dyes in visible light. Owing to their smaller optical band gap, Ag_2WO_4@MIL-125-NH_2@cotton and Ag_3VO_4@-MIL-125-NH_2@cotton composites showed the highest photodegradtion activity with achieving rate constant of 0.43–1.04 $\times$ 10^{-3} L/mg min and 0.29–0.79 10^{-3} L/mg min, respectively. The photocatalytic degradation of dyes in the presence of composites reduced to 58–65% for MB and 47–54% for RhB, by applying 4 recycling process.

Comparative with the photocatalysts in literature, the produced photocatalyst composites in the current work showed significant advantages represented in the ease control preparation technique, highly effective in daylight, applicable and recyclable. These feedbacks reflect the promising potency of the prepared photocatalyst composites in dye degradation, water treatment and in general environmental applications.

Compliance with ethical standards

Conflict of interest The authors declare that they have no conflict of interest.

References

Abdelhameed RM, El-Shahat M (2019) Fabrication of ZIF-67@MIL-125-NH2 nanocomposite with enhanced visible light photoreduction activity. J Environ Chem Eng 7(3):103194

Abdelhameed RM, Simões MM, Silva AM, Rocha J (2015) Enhanced photocatalytic activity of MIL-125 by post-synthetic modification with CrIII and Ag nanoparticles. Chemistry 21(31):11072–11081

Abdelhameed RM, Ananias D, Silva AMS, Rocha J (2017) Building light-emitting metal-organic frameworks by post-synthetic modification. ChemistrySelect 2(1):136–139

Abdelhameed RM, el-deib HR, El-Dars FM, Ahmed HB, Emam HE (2018a) Applicable strategy for removing liquid fuel nitrogenated contaminants using MIL-53-NH2@ natural fabric composites. Ind Eng Chem Res 57(44):15054–15065

Abdelhameed RM, Tobaldi DM, Karmaoui M (2018b) Engineering highly effective and stable nanocomposite photocatalyst based on NH2-MIL-125 encirclement with Ag_3PO_4 nanoparticles. J Photochem Photobiol A 351:50–58

Ahmed HB, Mikhail MM, El-Sherbiny S, Nagy KS, Emam HE (2020) pH responsive intelligent nano-engineer of nanostructures applicable for discoloration of reactive dyes. J Colloid Interface Sci 561:147–161

Alshammari A, Bagabas A, Assulami M (2014) Photodegradation of rhodamine B over semiconductor supported gold nanoparticles: the effect of semiconductor support identity. Arabian Journal of Chemistry

Balu S, Uma K, Pan G-T, Yang TC-K, Ramaraj SK (2018) Degradation of methylene blue dye in the presence of visible light using SiO_2@ α-Fe_2O_3 nanocomposites deposited on SnS_2 flowers. Materials 11(6):1030

Bhatkhande DS, Pangarkar VG, Beenackers AACM (2002) Photocatalytic degradation for environmental applications—a review. J Chem Technol Biotechnol 77(1):102–116

Bibi R, Shen Q, Wei L, Hao D, Li N, Zhou J (2018) Hybrid BiOBr/UiO-66-NH 2 composite with enhanced visible-light driven photocatalytic activity toward RhB dye degradation. RSC Adv 8(4):2048–2058

Burgeth G, Kisch H (2002) Photocatalytic and photoelectrochemical properties of titania–chloroplatinate (IV). Coord Chem Rev 230(1–2):41–47

Byrappa K, Subramani A, Ananda S, Rai KL, Dinesh R, Yoshimura M (2006) Photocatalytic degradation of rhodamine B dye using hydrothermally synthesized ZnO. Bull Mater Sci 29(5):433–438

Chekir N, Benhabiles O, Tassalit D, Laoufi NA, Bentahar F (2016) Photocatalytic degradation of methylene blue in aqueous suspensions using TiO_2 and ZnO. Desalin Water Treat 57(13):6141–6147

Chin M, Cisneros C, Araiza SM, Vargas KM, Ishihara KM, Tian F (2018) Rhodamine B degradation by nanosized zeolitic imidazolate framework-8 (ZIF-8). RSC Adv 8(47):26987–26997

Connell DW (2005) Basic concepts of environmental chemistry. CRC Press, Boca Raton

Connell DW, Miller GJ (1984) Chemistry and ecotoxicology of pollution, vol 65. Wiley, New York

Connell DW, Wu RS, Richardson BJ, Lam PK (2009) Chemistry of organic pollutants, including agrochemicals. Environ Ecol Chem 6:181

De Santana YV, Gomes JEC, Matos L, Cruvinel GH, Perrin A, Perrin C, Andrès J, Varela JA, Longo E (2014) Silver molybdate and silver tungstate nanocomposites with enhanced photoluminescence. Nanomater Nanotechnol 4:22

Di L, Yang H, Xian T, Liu X, Chen X (2019) Photocatalytic and photo-Fenton catalytic degradation activities of Z-scheme $Ag_2S/BiFeO_3$ heterojunction composites under visible-light irradiation. Nanomaterials 9(3):399

El-Dein AM, Libra J, Wiesmann U (2006) Cost analysis for the degradation of highly concentrated textile dye wastewater with chemical oxidation H_2O_2/UV and biological treatment. J Chem Technol Biotechnol 81(7):1239–1245

Emam HE, Bechtold T (2015) Cotton fabrics with UV blocking properties through metal salts deposition. Appl Surf Sci 357:1878–1889

Emam HE, Abdelhameed RM (2017) Anti-UV radiation textiles designed by embracing with nano-MIL (Ti, In)–metal organic framework. ACS Appl Mater Interfaces 9(33):28034–28045

Emam HE, Ahmed HB (2019) Comparative study between homo-metallic & hetero-metallic nanostructures based agar in catalytic degradation of dyes. Int J Biol Macromol 138:450–461

Emam HE, Shaheen TI (2019) Investigation into the role of surface modification of cellulose nanocrystals with succinic anhydride in dye removal. J Polym Environ 27(11):2419–2427

Emam HE, Abdellatif FH, Abdelhameed RM (2018) Cationization of celluloisc fibers in respect of liquid fuel purification. J Clean Prod 178:457–467

Emam HE, Saad NM, Abdallah AEM, Ahmed HB (2020) Acacia gum versus pectin in fabrication of catalytically active palladium nanoparticles for dye discoloration. Int J Biol Macromol 156:829–840

Forbes T (1993) Ecotoxicology in theory and practice. Springer, New York

Francis BM (1994) Toxic substances in the environment. Wiley, New York

Gajbhiye SB (2012) Photocatalytic degradation study of methylene blue solutions and its application to dye industry effluent. Int J Mod Eng Res 2(3):1204–1208

Gao H, Wang F, Wang S, Wang X, Yi Z, Yang H (2019) Photocatalytic activity tuning in a novel $Ag_2S/CQDs/CuBi_2O_4$ composite: synthesis and photocatalytic mechanism. Mater Res Bull 115:140–149

Garfield S (2002) Mauve: how one man invented a color that changed the world. WW Norton & Company, New York

Ghoreishi S, Haghighi R (2003) Chemical catalytic reaction and biological oxidation for treatment of non-biodegradable textile effluent. Chem Eng J 95(1–3):163–169

Hendon CH, Tiana D, Fontecave M, Sanchez C, D'arras L, Sassoye C, Rozes L, Mellot-Draznieks C, Walsh A (2013) Engineering the optical response of the titanium-MIL-125 metal–organic framework through ligand functionalization. J Am Chem Soc 135(30):10942–10945

Hu X, Hu C, Qu J (2008) Preparation and visible-light activity of silver vanadate for the degradation of pollutants. Mater Res Bull 43(11):2986–2997

Huang C-M, Pan G-T, Li Y-CM, Li M-H, Yang TC-K (2009) Crystalline phases and photocatalytic activities of hydrothermal synthesis Ag_3VO_4 and $Ag_4V_2O_7$ under visible light irradiation. Appl Catal A 358(2):164–172

Jones KC, De Voogt P (1999) Persistent organic pollutants (POPs): state of the science. Environ Pollut 100(1–3):209–221

Landis W, Sofield R, Yu M-H, Landis WG (2003) Introduction to environmental toxicology: impacts of chemicals upon ecological systems. CRC Press, Boca Raton

Liu B, Lin L, Yu D, Sun J, Zhu Z, Gao P, Wang W (2018) Construction of fiber-based $BiVO_4/SiO_2$/reduced graphene oxide (RGO) with efficient visible light photocatalytic activity. Cellulose 25(2):1089–1101

Liu C, Wang J, Yang S, Li X, Lin X (2019) Ag_3 PO_4 nanocrystals and gC 3 N 4 quantum dots decorated Ag_2 WO_4 nanorods: ternary nanoheterostructures for photocatalytic degradation of organic contaminants in water. RSC Adv 9(14):8065–8072

Ma J, Yu F, Zhou L, Jin L, Yang M, Luan J, Tang Y, Fan H, Yuan Z, Chen J (2012) Enhanced adsorptive removal of methyl orange and methylene blue from aqueous solution by alkali-activated multiwalled carbon nanotubes. ACS Appl Mater Interfaces 4(11):5749–5760

Medhi H, Bhattacharyya KG (2017) Kinetic and mechanistic studies on adsorption of Cu (II) in aqueous medium onto montmorillonite K10 and its modified derivative. New J Chem 41(22):13533–13552

Neena D, Kondamareddy KK, Bin H, Lu D, Kumar P, Dwivedi R, Pelenovich VO, Zhao X-Z, Gao W, Fu D (2018) Enhanced visible light photodegradation activity of RhB/MB from aqueous solution using nanosized novel Fe-Cd co-modified ZnO. Sci Rep 8(1):1–12

Panakoulias T, Kalatzis P, Kalderis D, Katsaounis A (2010) Electrochemical degradation of reactive red 120 using DSA and BDD anodes. J Appl Electrochem 40(10):1759–1765

Pica M, Calzuola S, Donnadio A, Gentili PL, Nocchetti M, Casciola M (2019) De-ethylation and cleavage of rhodamine B by a zirconium phosphate/silver bromide composite photocatalyst. Catalysts 9(1):3

Ramezani M, Pourmortazavi S, Sadeghpur M, Yazdani A, Kohsari I (2015) Silver tungstate nanostructures: electrochemical synthesis and its statistical optimization. J Mater Sci 26(6):3861–3867

Rasalingam S, Peng R, Koodali RT (2014) Removal of hazardous pollutants from wastewaters: applications of TiO_2-SiO_2 mixed oxide materials. J Nanomater

Ravi G, Reddy CS, Sreenu K, Guje R, Velchuri R, Vithal M (2016) Degradation of methylene blue and rhodamine B using a new visible light-responsive photocatalyst, KSb 2 PO 8–x N y. Acta Metall Sin 29(4):335–343

Seery MK, George R, Floris P, Pillai SC (2007) Silver doped titanium dioxide nanomaterials for enhanced visible light photocatalysis. J Photochem Photobiol A 189(2–3):258–263

Sitthichai S, Jonjana S, Phuruangrat A, Kuntalue B, Thongtem T, Thongtem S (2017) Photodegradation of rhodamine B by Ag_3PO_4/Bi_2MoO_6 nanocomposites under visible light illumination. J Ceram Soc Jpn 125(5):387–390

Soltani N, Saion E, Hussein MZ, Erfani M, Abedini A, Bahmanrokh G, Navasery M, Vaziri P (2012) Visible light-induced degradation of methylene blue in the presence of photocatalytic ZnS and CdS nanoparticles. Int J Mol Sci 13(10):12242–12258

Sreedevi A, Priyanka KP, Babitha KK, Sankararaman SI, Thomas V (2017) Synthesis and characterization of silver tungstate/iron phthalocyanine nanocomposite for electronic applications. Eur Phys J B 90(6):102

Suresh P, Umabala A, Rao AP (2015) Rapid sun light degradation of Rhodamine-B, Methylene blue, Methyl orange, Congo red and their binary mixtures using suprastoichiometric Bi-Molybdate. International J Eng Appl Sci 2 (8)

Vilela SM, Salcedo-Abraira P, Colinet I, Salles F, De Koning MC, Joosen MJ, Serre C, Horcajada P (2017) Nanometric MIL-125-NH_2 metal–organic framework as a potential nerve agent antidote carrier. Nanomaterials 7(10):321

Wang Y, Yu D, Wang W, Gao P, Zhang L, Zhong S, Liu B (2019) The controllable synthesis of novel heterojunction CoO/$BiVO_4$ composite catalysts for enhancing visible-light photocatalytic property. Colloids Surf A 578:123608

Wang Y, Ding K, Xu R, Yu D, Wang W, Gao P, Liu B (2020a) Fabrication of $BiVO_4/BiPO_4$/GO composite photocatalytic material for the visible light-driven degradation. J Clean Prod 247:119108

Wang Y, Yu D, Wang W, Gao P, Zhong S, Zhang L, Zhao Q, Liu B (2020b) Synthesizing Co_3O_4-$BiVO_4$/g-C3N4 heterojunction composites for superior photocatalytic redox activity. Sep Purif Technol 116562

Wankhade Atul V, Gaikwad G, Dhonde M, Khaty N, Thakare S (2013) Removal of organic pollutant from water by heterogenous photocatalysis: a review. Res J Chem Environ 17:84–94

Xiang W, Zhang Y, Lin H, Liu C-j (2017) Nanoparticle/metal–organic framework composites for catalytic applications: current status and perspective. Molecules 22(12):2103

Yang Q, Xu Q, Jiang H-L (2017) Metal–organic frameworks meet metal nanoparticles: synergistic effect for enhanced catalysis. Chem Soc Rev 46(15):4774–4808

Yang R, Zhu Z, Hu C, Zhong S, Zhang L, Liu B, Wang W (2020) One-step preparation (3D/2D/2D) $BiVO_4/FeVO_4$@ rGO heterojunction composite photocatalyst for the removal of tetracycline and hexavalent chromium ions in water. Chem Eng J 390:124522

Zhang T, Lin W (2014) Metal–organic frameworks for artificial photosynthesis and photocatalysis. Chem Soc Rev 43(16):5982–5993

Zhang C-F, Qiu L-G, Ke F, Zhu Y-J, Yuan Y-P, Xu G-S, Jiang X (2013) A novel magnetic recyclable photocatalyst based on a core–shell metal–organic framework Fe_3O_4@ MIL-100 (Fe) for the decolorization of methylene blue dye. J Mater Chem A 1(45):14329–14334

Zhang H, Yu D, Wang W, Gao P, Zhang L, Zhong S, Liu B (2019) Recyclable and highly efficient photocatalytic fabric of Fe (III)@ $BiVO_4$/cotton via thiol-ene click reaction with visible-light response in water. Adv Powder Technol 30(12):3182–3192

Zhao X, Huang J, Feng L, Cao L, Li J, Zhou L (2017) Facile synthesis of α-Ag3VO4 hollow nanospheres with improved photocatalytic activities. J Alloy Compd 718:7–14

Zhou Y, Zhang L, Cheng Z (2015) Removal of organic pollutants from aqueous solution using agricultural wastes: a review. J Mol Liq 212:739–762

Zhou T, Zhang G, Zhang H, Yang H, Ma P, Li X, Qiu X, Liu G (2018) Highly efficient visible-light-driven photocatalytic degradation of rhodamine B by a novel Z-scheme Ag_3PO_4/MIL-101/$NiFe_2O_4$ composite. Catal Sci Technol 8(9):2402–2416